Dimorphic $EuCu_5Cd$

Frank Tappe, Christian Schwickert and Rainer Pöttgen

Institut für Anorganische und Analytische Chemie, Universität Münster, Corrensstrasse 30, D-48149 Münster, Germany

Reprint requests to R. Pöttgen. E-mail: pottgen@uni-muenster.de

Z. Naturforsch. **2012**, *67b*, 1107 – 1114 / DOI: 10.5560/ZNB.2012-0109
Received April 24, 2012

Dedicated to Professor Heribert Offermanns on the occasion of his 75th birthday

Two modifications of $EuCu_5Cd$ were synthesized from the elements in sealed tantalum ampoules. The high-temperature (HT) modification was obtained from an induction-melted sample that was finally annealed at 873 K, while the low-temperature (LT) phase is formed in a muffle furnace by annealing a pre-melted sample at 673 K. DSC measurements gave a transition temperature of 823 ± 2 K. Both structures were refined on the basis of single-crystal X-ray diffractometer data: $R\bar{3}m$, $a = 511.58(7)$, $c = 3059.6(6)$ pm, $wR2 = 0.0289$, 316 F^2 values, 22 variables for HT-$EuCu_{4.85(1)}Cd_{1.15(1)}$ and $Pnma$, $a = 2545.6(5)$, $b = 511.60(1)$, $c = 1060.3(2)$ pm, $wR2 = 0.0386$, 2044 F^2 values, 121 variables for LT-$EuCu_{4.92(1)}Cd_{1.08(1)}$. A small degree of Cu/Cd mixing was observed for three sites. Both structures adopt new types. The europium atoms have high coordination numbers of 18, 19 and 20 in LT- and 18 and 20 in HT- $EuCu_5Cd$. These three types of polyhedra are the basic building units also in the closely related structures of $CeCu_6$, $CeCu_5Au$, $CeCu_{4.38}In_{1.62}$, and $CeNi_5Sn$, a family of stacking variants. Temperature-dependent magnetic susceptibility measurements of a HT- $EuCu_5Cd$ sample showed an experimental magnetic moment of 7.56(1) μ_B per Eu atom in the paramagnetic regime, compatible with divalent europium. HT- $EuCu_5Cd$ orders antiferromagnetically at 17.7(5) K.

Key words: Intermetallics, Cadmium, Dimorphism, Copper, Europium

Introduction

The rare earth (*RE*) transition metal (*T*) cadmium compounds display a large diversity of structural features [1]. However, in contrast to the $RE_xT_yMg_z$ [2] and especially $RE_xT_yZn_z$ [3] compounds, only few examples with larger cadmium content are known. Nevertheless, these few cadmium compounds show particularly interesting cadmium substructures. Isolated cadmium atoms (that means no Cd–Cd bonding) occur in the ordered Laves phases $RENi_4Cd$ [4], in the solid solutions $RE_{16}Rh_{11-x}Cd_x$ [5], in $Pr_6Fe_{13}Cd$ [6], or in EuAuCd [7]. In copper-rich $EuCu_9Cd_2$ [8] one observes the segregation of Cd_2 pairs with a Cd–Cd distance of 286 pm. These pairs are surrounded by the copper matrix. Infinite linear cadmium chains with shorter Cd–Cd distances of 273 pm have recently been observed in the solid solution $EuAu_{4+x}Cd_{2-x}$, in $CaAu_4Cd_2$ and in $SrAu_4Cd_2$ [9].

A lonsdaleite-related, orthorhombically distorted tetrahedral cadmium network (304 – 324 pm Cd–Cd) occurs in $LaNiCd_2$ [10]. This is one of the rare cadmium-rich examples [1]. Remarkable segregated Cd_4 tetrahedra have been observed in the rare earth-rich series RE_4TCd, $RE_{23}T_7Cd_4$ [1], and in the new structure type $La_{15}Rh_5Cd_2$ [11].

In continuation of our phase analytical work on such metal-rich cadmium intermetallics we obtained the new dimorphic compound $EuCu_5Cd$. The crystal chemical details and magnetic properties of this new phase are reported herein and compared to those of the complex structure types $CeCu_6$ [12], $CeCu_5Au$ [13], $CeCu_{4.38}In_{1.62}$ [14, 15], and $CeNi_5Sn$ [16].

Experimental

Synthesis

Starting materials for the preparation of both modifications of $EuCu_5Cd$ were sublimed ingots of europium (Johnson Matthey), copper shots (Johnson Matthey), and a cadmium rod (Johnson Matthey), all with stated purities better than 99.9 %. The larger europium ingots were cut into

smaller pieces in a glove box and kept under dry argon in Schlenk tubes prior to the reactions. The argon was purified with titanium sponge (900 K), silica gel, and molecular sieves. Pieces of the three elements were then weighed in the ideal 1 : 5 : 1 atomic ratio and arc-welded [17] in small tantalum ampoules under an argon atmosphere of *ca.* 800 mbar. For preparation of the low-temperature (LT) phase the tantalum tube was sealed in an evacuated silica tube for oxidation protection, placed in a muffle furnace and first heated to 1373 K within two hours. The temperature was kept for another four hours. Subsequently the furnace was cooled to 673 K within four days and then kept at that temperature for another four days followed by quenching. The tantalum tube for the preparation of the high-temperature (HT) phase was placed in the water-cooled sample chamber of an induction furnace [18] (Hüttinger Elektronik, Freiburg/Germany, Typ TIG 2.5/300), rapidly heated to 1373 K, and kept at that temperature for 5 min. The tube was then rapidly cooled to 873 K and annealed at that temperature for another three hours, followed by quenching by switching off the power supply. The temperature was controlled by a Sensor Therm Methis MS09 pyrometer with an accuracy of ±30 K. After both heat treatments, the brittle polycrystalline $EuCu_5Cd$ samples could easily be separated from the tantalum containers. No reactions with the crucible material were observed. The samples are stable in air over months. Single crystals have light-yellow metallic lustre; ground powders are dark gray.

EDX data

The $EuCu_5Cd$ single crystals studied on the diffractometer were investigated by semiquantitative EDX analyses by use of a Zeiss EVO MA10 scanning electron microscope (variable pressure mode) with EuF_3, Cu, and Cd as standards. The experimentally observed compositions were in good agreement with the ones obtained from the structure refinements (14 ± 2 at.-% Eu : 73 ± 2 at.-% Cu : 13 ± 2 at.-% Cd *vs.* 14.3 : 70.3 : 15.4 for LT-$EuCu_5Cd$ and 14 ± 2 at.-% Eu : 68 ± 2 at.-% Cu : 18 ± 2 at.-% Cd *vs.* 14.3 : 69.3 : 16.4 for HT-$EuCu_5Cd$). The standard deviations account for the irregular surface of the crystals. No impurity elements were found.

X-Ray diffraction

The polycrystalline samples of both $EuCu_5Cd$ modifications were characterized by powder X-ray diffraction: Guinier camera (imaging plate detector, Fujifilm BAS-1800 readout system), Cu K_{α_1} radiation and α-quartz ($a = 491.30$; $c = 540.46$ pm) as the internal standard. The lattice parameters (Table 1) were refined with a standard least-squares procedure. The correct indexing was ensured by intensity calculations [19]. The powder pattern of the LT-phase showed some additional reflections which could be assigned to a small remaining part of the HT-phase and $EuCu_9Cd_2$ [8].

Well-shaped single crystals of both modifications were selected from the crushed annealed samples. The crystals were glued to thin quartz fibres and their quality was first checked by Laue photographs on a Buerger camera (white Mo radiation). Intensity data were collected at room temperature by use of a Stoe IPDS-II imaging plate diffractometer in oscillation mode (graphite-monochromatized Mo K_α radiation). Numerical absorption corrections were applied to the data sets. The relevant details concerning the data collections and evaluations are listed in Table 2.

Structure refinements

The structure of LT-$EuCu_5Cd$ was investigated first. The data set showed a primitive orthorhombic lattice with high Laue symmetry and with systematic extinctions compatible with space group *Pnma*. The starting atomic parameters were determined *via* Direct Methods with SHELXS-97 [20], and the structure was refined using SHELXL-97 [21] (full-matrix least-squares on F^2) with anisotropic atomic displacement parameters for all sites. During the refinement procedure we observed too low displacement parameters for two of the copper sites, indicating higher scattering power, *i. e.* mixed occupancy with cadmium. All other sites were fully occupied within two standard deviations. In the subsequent cycles the two mixed occupancies were refined as least-squares variables, leading to the composition $EuCu_{4.92(1)}Cd_{1.08(1)}$

Table 1. Lattice parameters of the two modifications of $EuCu_5Cd$ and some related intermetallic compounds.

Structure	a (pm)	b (pm)	c (pm)	V (nm^3)/Z	Space group	Reference
$CeCu_6$	811.2(1)	510.2(1)	1016.2(5)	0.4206/4	*Pnma*	[12]
$CeCu_5Au$	824.55(4)	508.66(3)	1036.59(5)	0.4348/4	*Pnma*	[13]
$CeCu_{4.48}In_{1.62}$	1716.9(6)	520.2(2)	1090.8(4)	0.9742/8	*Pnmn*	[14, 15]
LT-$EuCu_5Cd$	2545.8(8)	511.7(1)	1060.5(4)	1.3815/12	*Pnma*	This work
LT-$EuCu_{4.92}Cd_{1.08}$[a]	2545.6(5)	511.60(1)	1060.3(2)	1.3809/12	*Pnma*	This work
$CeNi_5Sn$	490.49(4)	*a*	1973.1(2)	0.4111/4	$P6_3/mmc$	[16]
HT-$EuCu_5Cd$	511.8(1)	*a*	3056.9(9)	0.6934/6	$R\bar{3}m$	This work
HT-$EuCu_{4.85}Cd_{1.15}$	511.58(7)	*a*	3059.6(6)	0.6935/6	$R\bar{3}m$	This work

[a] Single crystal data.

Table 2. Crystal data and structure refinement for HT-$EuCu_{4.85(1)}Cd_{1.15(1)}$ and LT-$EuCu_{4.92(1)}Cd_{1.08(1)}$.

Empirical formula	HT-$EuCu_{4.85(1)}Cd_{1.15(1)}$	LT-$EuCu_{4.92(1)}Cd_{1.08(1)}$
Unit cell dimensions	Table 1	Table 1
Molar mass, g mol^{-1}	589.47	585.89
Calculated density, g cm^{-3}	8.47	8.46
Space group	$R\bar{3}m$	*Pnma*
Formula units per cell, Z	6	12
Crystal size, μm^3	$10 \times 20 \times 40$	$20 \times 40 \times 40$
Transm. ratio (max/min)	0.813/0.386	0.616/0.253
Absorption coeff., mm^{-1}	40.2	40.4
Detector distance, mm	90	100
Exposure time, min	7	6
ω range; increment, deg	0 – 180°; 1.0°	0 – 180°; 1.0°
Integr. param. A; B; EMS	12.8; 2.8; 0.012	12.3; 2.3; 0.011
$F(000)$, e	1553	3090
θ range, deg	2–31	1–30
Range in *hkl*	±7, ±7, ±43	±34, ±7, ±14
Total no. reflections	2699	13 238
Independent reflections/R_{int}	316/0.0254	2044/0.0669
Reflections with $I > 2\sigma(I)/R_\sigma$	261/0.0204	957/0.0850
Data/ref. parameters	316/22	2044/121
Goodness-of-fit on F^2	1.036	0.677
$R1/wR2$ for $I > 2\sigma(I)$	0.0190/0.0275	0.0247/0.0322
$R1/wR2$ for all data	0.0308/0.0289	0.0941/0.0386
Extinction coefficient	0.00038(5)	0.000190(11)
Largest diff. peak/hole, e Å^{-3}	1.40/ – 1.02	1.29/ – 1.38

for the investigated crystal. The data set of the HT-phase showed a hexagonal unit cell and the systematic extinctions were compatible with the rhombohedral space group $R\bar{3}m$. During this structure refinement we also observed one mixed-occupied site, and the refined composition was $EuCu_{4.85(1)}Cd_{1.15(1)}$. The final difference Fourier syntheses were flat (Table 2). The positional parameters and interatomic distances are listed in Tables 3–5.

Further details of the crystal structure investigation may be obtained from Fachinformationszentrum Karlsruhe, 76344 Eggenstein-Leopoldshafen, Germany (fax: +49-7247-808-666; e-mail: crysdata@fiz-karlsruhe.de, http://www.fiz-karlsruhe.de/request_for_deposited_data.html) on quoting the deposition numbers CSD-424588 (LT-$EuCu_5Cd$) and CSD-424589 (HT-$EuCu_5Cd$).

Magnetic susceptibility measurements

Pieces of the HT-$EuCu_5Cd$ sample were enclosed in kapton foil and attached to the sample holder rod of a VSM for measuring the magnetic properties in a Quantum Design Physical-Property-Measurement System in the temperature range of 3 – 300 K with magnetic flux densities up to 80 kOe.

Discussion

Crystal chemistry

Both modifications of $EuCu_5Cd$ crystallize with new structure types, *i. e.* *Pnma*, oP84 for LT-$EuCu_5Cd$ and $R\bar{3}m$, hR42 for HT-$EuCu_5Cd$. A common feature for both phases is the mixed Cu/Cd occupancy of one and two copper sites, respectively (Table 3). In order to obtain data on the phase transition temperature, the $EuCu_5Cd$ samples were studied by differential thermal analysis (DTA; Netzsch STA 409 C/CD) and also by differential scanning calorimetry (DSC; Netzsch DSC 204 *Phoenix*). The phase transition is reversible and the transition temperature was determined to be 823 ± 2 K (Fig. 1). Thus, we have real dimorphism and not two phases that adopt different structures as a function of the composition, caused by the mixed occupancies.

The europium atoms in both phases have high coordination numbers, *i. e.* 18, 19, and 20 in the low-, and 18 and 20 in the high-temperature phase (Fig. 2). Although we observe triangular faces within the europium polyhedra, these units do not belong to the class of Frank-Kasper polyhedra [22, 23]. These polyhedra (named A, B, and C) are the basic building units, and the two structures can be constructed by different stackings of these polyhedra. A literature search readily gave the structurally closely related phases $CeCu_6$ [12], $CeCu_5Au$ [13], $CeCu_{4.38}In_{1.62}$ [14, 15], and $CeNi_5Sn$ [16]. The different stacking variants of the polyhedra A, B, and C are presented in Fig. 3.

Table 3. Atomic coordinates and equivalent isotropic displacement parameters of HT-$EuCu_{4.85(1)}Cd_{1.15(1)}$ and LT-$EuCu_{4.92(1)}Cd_{1.08(1)}$.

Atom	Wyckoff site	x	y	z	U_{eq}
HT-$EuCu_{4.85(1)}Cd_{1.15(1)}$					
Eu1	3*b*	0	0	1/2	150(2)
Eu2	3*a*	0	0	0	120(2)
Cu1	18*h*	0.49952(8)	$-x$	0.06781(2)	123(2)
85(1)% Cu2	6*c*	0	0	0.19813(4)	177(5)
15(1)% Cd2					
Cu3	6*c*	0	0	0.33398(4)	137(2)
Cd1	6*c*	0	0	0.11009(2)	138(2)
LT-$EuCu_{4.92(1)}Cd_{1.08(1)}$					
Eu1	4*c*	0.08395(4)	1/4	0.55839(10)	131(2)
Eu2	4*c*	0.24744(4)	1/4	0.18106(7)	143(2)
Eu3	4*c*	0.41601(4)	1/4	0.55907(10)	158(2)
Cu1	8*d*	0.18964(6)	−0.0001(3)	0.42979(12)	138(3)
Cu2	8*d*	0.35568(5)	0.0017(3)	0.30343(13)	142(3)
Cu3	8*d*	0.97754(5)	0.0008(3)	0.68756(13)	140(3)
88(2)% Cu4	4*c*	0.01685(9)	1/4	0.1060(2)	181(8)
12(2)% Cd4					
89(2)% Cu5	4*c*	0.14952(8)	1/4	0.00835(18)	174(8)
11(2)% Cd5					
Cu6	4*c*	0.19640(8)	1/4	0.6334(2)	151(5)
Cu7	4*c*	0.22783(8)	1/4	0.85968(19)	140(4)
Cu8	4*c*	0.31562(9)	1/4	0.7257(2)	155(4)
Cu9	4*c*	0.35996(9)	1/4	0.0994(2)	156(5)
Cu10	4*c*	0.39432(8)	1/4	0.87035(19)	144(4)
Cu11	4*c*	0.43887(8)	1/4	0.24549(19)	140(4)
Cu12	4*c*	0.47200(9)	1/4	0.0172(2)	151(4)
Cd1	4*c*	0.11949(5)	1/4	0.25398(13)	148(3)
Cd2	4*c*	0.28723(5)	1/4	0.48040(12)	137(3)
Cd3	4*c*	0.54686(5)	1/4	0.63723(12)	150(3)

Table 4. Interatomic distances (pm) in the structure of HT-$EuCu_{4.85(1)}Cd_{1.15(1)}$. All distances within the first coordination spheres are listed. Standard deviations are all equal or smaller than 0.2 pm.

Eu1:	6	Cu2/Cd	310.7	Cu2/:	3	Cu1	253.9
	6	Cu1	336.4	Cd2	1	Cd1	269.4
	6	Cd1	342.4		3	Cd1	305.2
Eu2:	6	Cu3	295.4		3	Eu1	310.7
	12	Cu1	329.4		3	Cu2/Cd2	352.6
	2	Cd1	336.8	Cu3:	3	Cu1	252.8
Cu1:	1	Cu3	252.8		3	Cu1	256.5
	1	Cu2/Cd2	253.9		3	Eu2	295.4
	2	Cu1	255.1		3	Cu3	295.4
	1	Cu3	256.5	Cd1:	1	Cu2/Cd2	269.4
	2	Cu1	256.5		6	Cu1	286.6
	2	Cd1	286.6		3	Cu2/Cd2	305.2
	2	Eu2	329.4		1	Eu2	336.8
	1	Eu1	336.4		3	Eu1	342.4

$CeCu_6$ and its ternary ordered version $CeCu_5Au$ are built up only from the polyhedron type A, while all three types of polyhedra are present in $CeCu_{4.38}In_{1.62}$ and LT-$EuCu_5Cd$, however, with a different connectivity pattern. Only polyhedra of types B and C occur in the structures of $CeNi_5Sn$ and HT-$EuCu_5Cd$. The stacking sequences *ABAB* of the polyhedral layers in $CeNi_5Sn$ leads to a hexagonal, and the *ABCABC* ordering in HT-$EuCu_5Cd$ to a rhombohedral structure. Considering simply the unit cell dimensions and the space group symmetry, at first sight one might think of an isomorphic superstructure i3 (which is allowed for space group *Pnma*) of $CeCu_5Au$ for LT-$EuCu_5Cd$. This is not the case and the two structures are only related by the stacking pattern.

Comparing Tables 4 and 5 makes it readily evident that most interatomic distances in the structures of LT-$EuCu_5Cd$ and HT-$EuCu_5Cd$ are in the same ranges. The shortest distances in both modifications occur for Cu–Cu. They range from 251 to 298 pm in LT-$EuCu_5Cd$ and from 252 to 257 pm in HT-$EuCu_5Cd$. These distances are all close to the Cu–Cu distance of 256 pm in fcc copper [24]. The Cu–Cd distances (269 – 305 pm in LT-$EuCu_5Cd$ and 269 – 306 pm in HT-$EuCu_5Cd$) are slightly longer than the sum of the covalent radii [25] of 258 pm, indicating weaker Cu–

Table 5. Interatomic distances (pm) in the structure of LT-$EuCu_{4.92(1)}Cd_{1.08(1)}$. All distances within the first coordination spheres are listed. Standard deviations are all equal or smaller than 0.3 pm.

Eu1:	2	Cu12	296.0	Cu2:	1	Cu9	251.1	Cu6:	2	Cu1	251.6	Cu11:	1	Cu4/Cd4	253.4
	1	Cu12	296.1		1	Cu5/Cd5	252.9		1	Cu7	252.9		1	Cu9	253.7
	2	Cu9	296.2		1	Cu2	254.0		2	Cu2	258.2		2	Cu2	254.5
	1	Cu6	297.1		1	Cu11	254.5		1	Cd2	282.5		2	Cu3	255.9
	2	Cu1	327.7		1	Cu7	255.6		2	Cu9	295.5		1	Cu12	256.3
	2	Cu2	328.2		1	Cu2	257.6		1	Eu1	297.1		2	Cd3	286.7
	2	Cu11	328.9		1	Cu6	258.2		2	Eu2	297.4		2	Eu1	328.9
	2	Cu10	329.0		1	Cd2	285.8		1	Cu8	318.9		1	Eu3	337.5
	2	Cu3	329.2		1	Cd3	286.5	Cu7:	1	Cu6	252.9	Cu12:	1	Cu10	251.7
	2	Cu3	330.1		1	Eu1	328.2		1	Cu5/Cd5	254.1		2	Cu3	252.2
	1	Cd1	335.2		1	Eu2	330.0		2	Cu2	255.6		2	Cu3	256.1
	1	Cd3	336.3		1	Eu3	336.4		2	Cu1	256.9		1	Cu11	256.3
Eu2:	2	Cu6	297.4	Cu3:	1	Cu12	252.2		1	Cu8	264.8		2	Cu12	295.1
	1	Cu9	299.2		1	Cu4/Cd4	254.1		2	Cd2	288.6		2	Eu1	296.0
	2	Cu8	305.7		1	Cu10	254.8		2	Eu2	324.4		1	Eu1	296.1
	1	Cu5/Cd5	309.3		1	Cu3	255.0		1	Eu2	344.4		1	Cu9	298.2
	2	Cu7	324.4		1	Cu11	255.9	Cu8:	2	Cu1	251.7	Cd1:	1	Cu5/Cd5	271.4
	2	Cu1	328.0		1	Cu12	256.1		1	Cu10	252.3		2	Cu3	285.2
	2	Cu2	330.0		1	Cu3	256.6		1	Cu7	264.8		2	Cu10	286.2
	1	Cd2	333.2		1	Cd1	285.2		1	Cd2	269.9		2	Cu1	288.1
	1	Cd1	334.8		1	Cd3	286.2		2	Eu2	305.7		1	Cu4/Cd4	304.8
	2	Cu1	336.1		1	Eu1	329.2		2	Cd1	306.0		2	Cu8	306.0
	2	Cd2	344.2		1	Eu1	330.1		1	Eu3	310.7		1	Eu2	334.8
	1	Cu7	344.4		1	Eu3	336.1		1	Cu6	318.9		1	Eu1	335.2
Eu3:	2	Cu5/Cd5	310.1	Cu4/:	1	Cu11	253.4		2	Cu5/Cd5	355.5		2	Eu3	341.1
	1	Cu8	310.7	Cd4	2	Cu3	254.1	Cu9:	2	Cu2	251.1	Cd2:	1	Cu8	269.9
	1	Cu4/Cd4	310.7		1	Cd3	269.0		1	Cu11	253.7		1	Cu6	282.5
	2	Cu4/Cd4	311.6		2	Cd3	304.7		2	Cu1	254.2		2	Cu1	284.5
	1	Cu10	334.6		1	Cd1	304.8		1	Cu10	258.1		2	Cu2	285.8
	2	Cu3	336.1		1	Eu3	310.7		2	Cu6	295.5		2	Cu7	288.6
	2	Cu2	336.4		2	Eu3	311.6		2	Eu1	296.2		2	Cu5/Cd5	303.7
	1	Cu11	337.5		2	Cu4/Cd4	351.1		1	Cu12	298.2		1	Eu2	333.2
	1	Cd2	338.3		1	Cu5/Cd5	353.2		1	Eu2	299.2		1	Eu3	338.3
	2	Cd1	341.1	Cu5/:	2	Cu2	252.9	Cu10:	1	Cu12	251.7		2	Eu2	344.2
	2	Cd3	343.1	Cd5	1	Cu7	254.1		1	Cu8	252.3	Cd3:	1	Cu4/Cd4	269.0
	1	Cd3	343.3		1	Cd1	271.4		2	Cu3	254.8		2	Cu3	286.2
Cu1:	1	Cu6	251.6		1	Cd3	303.5		2	Cu1	256.9		2	Cu2	286.5
	1	Cu8	251.7		2	Cd2	303.7		1	Cu9	258.1		2	Cu11	286.7
	1	Cu9	254.2		1	Eu2	309.3		2	Cd1	286.2		1	Cu5/Cd5	303.5
	1	Cu1	255.7		2	Eu3	310.1		2	Eu1	329.0		2	Cu4/Cd4	304.7
	1	Cu1	255.9		1	Cu4/Cd4	353.2		1	Eu3	334.6		1	Eu1	336.3
	1	Cu10	256.9		2	Cu8	355.5						2	Eu3	343.1
	1	Cu7	256.9										1	Eu3	343.3
	1	Cd2	284.5												
	1	Cd1	288.1												
	1	Eu1	327.7												
	1	Eu2	328.0												
	1	Eu2	336.1												

Cd bonding. Similar to the structure of Eu_5Cu_2Cd (321 – 335 pm Eu–Cu) [26], the europium atoms in LT- and HT- $EuCu_5Cd$ have their shortest bonds also to the copper atoms.

Finally we need to comment on the structures of Sr_5Al_9 [27] and K_5InPb_8 [28] which also crystallizes in space group $R\bar{3}m$ with the Wyckoff sequence 166, hc^3ba. At first sight one might think that the aluminide and the plumbide are isotypic with HT-$EuCu_5Cd$, however, the z parameter of the 18h sites in HT- $EuCu_5Cd$ is distinctly different, leading to dissimilar coordinations.

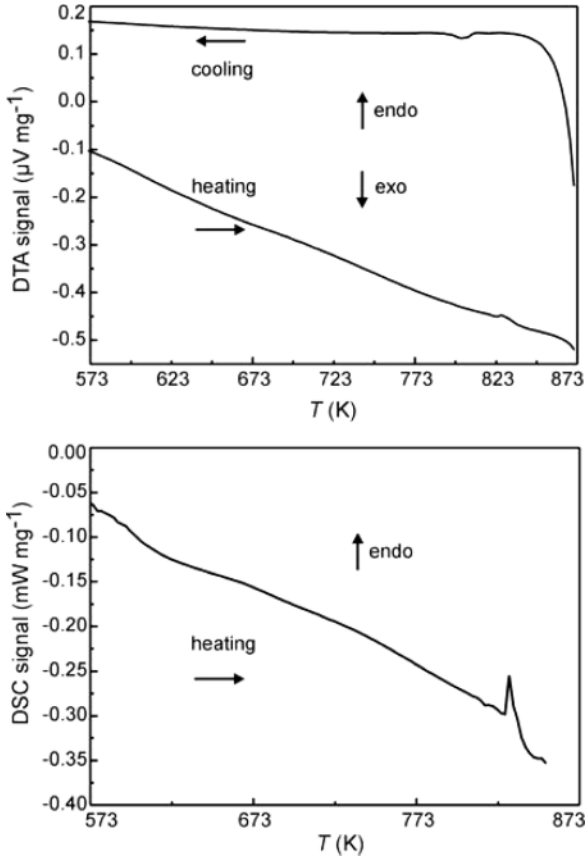

Fig. 1. Differential thermal analyses (DTA) (top) and differential scanning calorimetry (DSC) (bottom) of $EuCu_5Cd$.

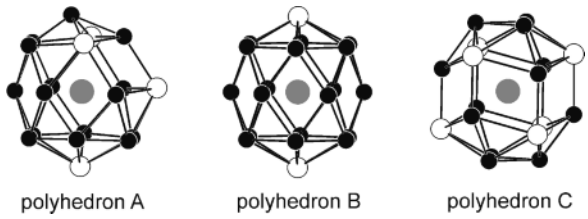

Fig. 2. Coordination polyhedra of the three crystallographically independent europium atoms in LT-$EuCu_5Cd$. Europium, copper, and cadmium atoms are drawn as medium grey, black filled, and open circles, respectively. For simplicity, the mixed-occupied sites are drawn as pure copper atoms. (polyhedron A ≡ Eu2; polyhedron B ≡ Eu1; polyhedron C ≡ Eu3).

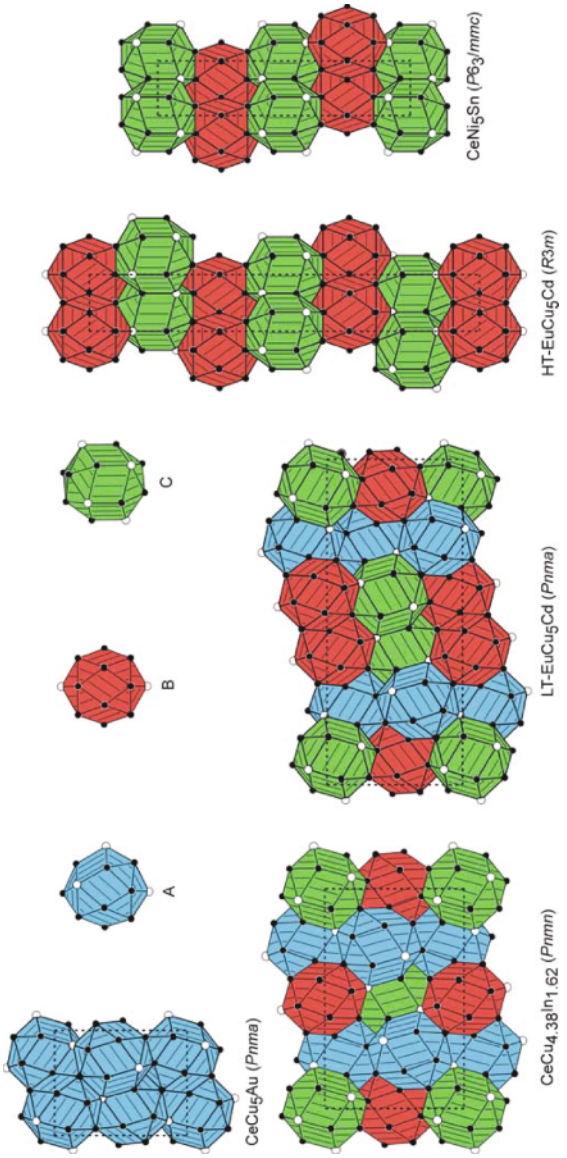

Fig. 3 (color online). The crystal structures of $CeCu_5Au$, $CeCu_{4.38}In_{1.62}$, LT-$EuCu_5Cd$, HT-$EuCu_5Cd$, and $CeNi_5Sn$ as projections along the short unit cell axis. The $CeCu_{4.38}In_{1.62}$ structure is drawn in the non-standard *Pnmn* setting in order to facilitate comparison with the other structure types. The three different types of polyhedra shown in Fig. 3 are drawn in blue, red, and green color. For details see text.

Magnetic properties of HT-$EuCu_5Cd$

Only the high-temperature phase was obtained in pure form. The temperature dependence of the magnetic susceptibility measured at 10 kOe is presented in Fig. 4 (top). HT-$EuCu_5Cd$ shows Curie-Weiss behavior in the temperature regime 100 – 300 K and the experimental magnetic moment was determined

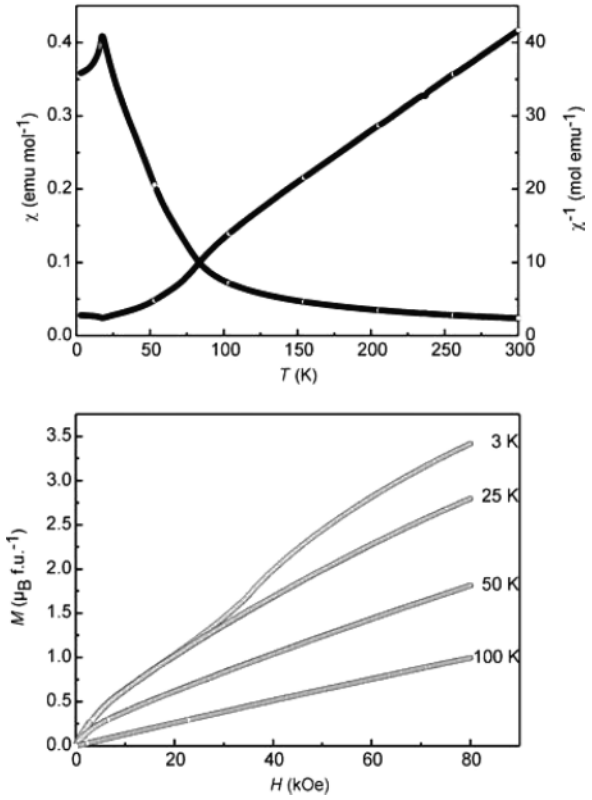

Fig. 4. Temperature dependence of the magnetic susceptibility (χ and χ^{-1} data) (top) and magnetization isotherms (bottom) of HT-$EuCu_5Cd$.

as 7.56(1) μ_B per Eu atom, compatible with divalent europium. Extrapolation of the χ^{-1} *vs.* T plot showed a Weiss constant of 10.7(5) K. Below 100 K we observe a small bump in the susceptibility plot which is associated with a trace amount of a ferromagnetic ($T_C = 70$ K) EuO impurity, frequently observed in europium intermetallics [29], most recently also for Eu_5Au_2Cd [26]. The europium magnetic moments in HT-$EuCu_5Cd$ order antiferromagnetically at $T_N = 17.7(5)$ K.

The magnetization behavior of HT-$EuCu_5Cd$ is presented in Fig. 4 (bottom). At 100 K, well above the magnetic ordering temperatures of HT-$EuCu_5Cd$ and EuO, we observe a linear increase of the magnetization as expected for a paramagnetic material. The 50 K magnetization isotherm already shows a small curvature at low fields, a result of the small ferromagnetic EuO impurity, similar to the 25 K data. At 3 K, well below the Néel temperature of HT-$EuCu_5Cd$, we observe a weak metamagnetic step (antiferromagnetic-to-ferromagnetic spin reorientation) at a critical field of 36 kOe. This field-induced reorientation fully underlines the antiferromagnetic ground state of HT-$EuCu_5Cd$. The maximum magnetization observed at 3 K and 80 kOe is 3.42(5)μ_B per Eu atom, much smaller than the theoretical value of 7μ_B according to $g \times S$. Full parallel spin alignment is thus acchieved at much higher external fields.

Acknowledgement

We thank Dipl.-Ing. U. Ch. Rodewald for the intensity data collections and W. Pröbsting for the DTA/DSC data. This work was financially supported by the Deutsche Forschungsgemeinschaft.

[1] F. Tappe, R. Pöttgen, *Rev. Inorg. Chem.* **2011**, *31*, 5.
[2] U. Ch. Rodewald, B. Chevalier, R. Pöttgen, *J. Solid State Chem.* **2007**, *180*, 1720.
[3] P. Villars, K. Cenzual, Pearson's Crystal Data: Crystal Structure Database for Inorganic Compounds (release 2011/12), ASM International®, Materials Park, Ohio (USA) **2011**.
[4] F. Tappe, C. Schwickert, R. Pöttgen, *Intermetallics* **2012**, *24*, 33.
[5] F. Tappe, F. M. Schappacher, T. Langer, I. Schellenberg, R. Pöttgen, *Z. Naturforsch.* **2012**, *67b*, 594.
[6] F. Weitzer, A. Leithe-Jasper, P. Rogl, K. Hiebl, A. Rainbacher, G. Wiesinger, W. Steiner, J. Friedl, F. E. Wagner, *J. Appl. Phys.* **1994**, *75*, 7745.
[7] R. Mishra, R. Pöttgen, R.-D. Hoffmann, D. Kaczorowski, H. Piotrowski, P. Mayer, C. Rosenhahn, B. D. Mosel, *Z. Anorg. Allg. Chem.* **2001**, *627*, 1283.
[8] F. Tappe, C. Schwickert, R. Pöttgen, *Z. Anorg. Allg. Chem.* **2012**, *638*, in press, 2012.
[9] F. Tappe, S. F. Matar, C. Schwickert, F. Winter, R. Pöttgen, *Monatsh. Chem.*, submitted for publication, 2012.
[10] A. Doğan, D. Johrendt, R. Pöttgen, *Z. Anorg. Allg. Chem.* **2005**, *631*, 451.
[11] F. Tappe, U. Ch. Rodewald, R.-D. Hoffmann, R. Pöttgen, *Z. Naturforsch.* **2011**, *66b*, 559.
[12] D. T. Cromer, A. C. Larson, R. B. Roof, Jr., *Acta Crystallogr.* **1960**, *13*, 913.

[13] M. Ruck, G. Portisch, H. G. Schlager, M. Sieck, H. von Löhneysen, *Acta Crystallogr.* **1993**, *B49*, 936.
[14] Ya. M. Kalychak, V. M. Baranyak, V. M. Belsky, O. V. Dmytrakh, *Dopov. Akad. Nauk. Ukr. RSR, Ser. B* **1988**, *9*, 39.
[15] S. Bobev, E. D. Bauer, *Acta Crystallogr.* **2005**, *E61*, i89.
[16] R. V. Skolozdra, V. M. Mandzyk, L. G. Akselrud, *Sov. Phys. Crystallogr.* **1981**, *26*, 272.
[17] R. Pöttgen, Th. Gulden, A. Simon, *GIT Labor-Fachzeitschrift* **1999**, *43*, 133.
[18] R. Pöttgen, A. Lang, R.-D. Hoffmann, B. Künnen, G. Kotzyba, R. Müllmann, B. D. Mosel, C. Rosenhahn, *Z. Kristallogr.* **1999**, *214*, 143.
[19] K. Yvon, W. Jeitschko, E. Parthé, *J. Appl. Crystallogr.* **1977**, *10*, 73.
[20] G. M. Sheldrick, SHELXS-97, Program for the Solution of Crystal Structures, University of Göttingen, Göttingen (Germany) **1997**. See also: G. M. Sheldrick, *Acta Crystallogr.* **1990**, *A46*, 467.
[21] G. M. Sheldrick, SHELXL-97, Program for the Refinement of Crystal Structures, University of Göttingen, Göttingen (Germany) **1997**. See also: G. M. Sheldrick, *Acta Crystallogr.* **2008**, *A64*, 112.
[22] F. C. Frank, J. S. Kasper, *Acta Crystallogr.* **1958**, *11*, 184.
[23] F. C. Frank, J. S. Kasper, *Acta Crystallogr.* **1959**, *12*, 483.
[24] J. Donohue, *The Structures of the Elements*, Wiley, New York **1974**.
[25] J. Emsley, *The Elements*, Oxford University Press, Oxford **1999**.
[26] F. Tappe, C. Schwickert, M. Eul, R. Pöttgen, *Z. Naturforsch.* **2011**, *66b*, 1219.
[27] M. B. Manyako, O. S. Zarechnyuk, T. I. Yanson, *Sov. Phys. Crystallogr.* **1987**, *32*, 196.
[28] M. T. Klem, J. D. Corbett, *Inorg. Chem.* **2005**, *44*, 5990.
[29] R. Pöttgen, D. Johrendt, *Chem. Mater.* **2000**, *12*, 875.